Slovak Society of Chemical Engineering

Institute of Chemical and Environmental Engineering

Slovak University of Technology in Bratislava

PROCEEDINGS

37th International Conference of Slovak Society of Chemical Engineering

Hotel Hutník

Tatranské Matliare, Slovakia

May 24 – 28, 2010

Editor: J. Markoš

ISBN 978-80-227-3290-1

Jugovic, B., Trisovic, T., Stevanovic, J., Gvozdenovic, M., Grgur, B.: Improved electrolyte for zinc-polyaniline batteries, Editor: Markoš, J., In *Proceedings of the 37th International Conference of Slovak Society of Chemical Engineering*, Tatranské Matliare, Slovakia, 866–870, 2010.

Improved electrolyte for zinc-polyaniline batteries

B.Z. Jugović[1], T. Lj. Trišović[1], J. Stevanović[2], M. Gvozdenović[3], B.N. Grgur[3]
[1]*Institute of Technical Science, Serbian Academy of Science and Arts, Knez Mihailova 35, Belgrade*
[2]*Institute of Electrochemistry, ICTM, Njegoševa 12 Belgrade*
[3]*Faculty of Technology and Metallurgy, Karnegijeva 4, Belgrade*

Electrochemical behavior of zinc and polyaniline (PANI) electrode polymerized from 0.1 M HCl and 0.1 M aniline on graphite electrode, in 0.2 M $ZnCl_2$ and 0.50 M NH_4Cl (chloride electrolyte) and with addition of 0.33 M Na-citrate (chloride/citrate electrolyte) were investigated. In the chloride/citrate comparing with chloride containing electrolyte for the zinc electrode negative shift of the open circuit potential of 150 mV, decreases of exchange current density for more than order of magnitude and increase of cathodic Tafel slope, due to the zinc ions complexation, were observed. In citrate/chloride electrolyte zinc dendrite formation were completely suppressed. PANI electrodes show better discharge characteristic in chloride/citrate electrolyte with determined maximum discharge capacity of 164 mAh g^{-1}

Key words: polyaniline, citrate, batteries

1. Introduction

Up to now zinc-PANI batteries has not been commercialized from few main reasons. First reason is degradation process of PANI at potentials more positive than ~0.5 V [1, 2], and second is zinc passivation, which is possibly related to the formation of the solid phases $ZnCl_2 \cdot 3NH_4Cl$ and $ZnCl_2 \cdot 2NH_4Cl$ on the anode surface [3]. On the other hand, in chloride containing electrolytes Zn electrodes form dendrites during charge–discharge cycles [5]. It results in decreased coulombic efficiency of batteries and charge life. Main reason for that are sort circuit provoked by penetration of dendrites through separator to cathode or formation of the anodic slime.

It is well known that some organic anions can form complexes with the metal ions, that results much better quality of the metal deposits and suppress dendrite formation [7]. Probably, the best choice will be oxalic anions, due to the small ionic radius, good PANI doping-dedoping characteristics, etc [8]. Unfortunately, zinc oxalate is an insoluble salt.

In this paper we have investigated behavior of zinc and PANI electrodes in chloride containing electrolytes with addition of citrate anions, which at pH~5 that can form an soluble zinc citrate $[ZnCit]^-$ complex.

2. Experimental

Polyaniline was obtained from hydrochloric acid solution (0.1 M) with addition of 0.1 M aniline monomer (p.a. Merck, distilled in argon atmosphere), at constant current density of 1 mA cm^{-2} on graphite electrode. Electrolytes containing 0.5 M NH_4Cl, 0.20 M $ZnCl_2$ and with addition of 0.33 M Na-citrate were prepared from p.a. grade chemicals (Merck) and bidistiled water. For all experiments three compartment electrochemical cell, with platinum foil (S=2 cm^2) as a counter and saturated calomel electrode as a reference electrode at room temperature was used.

The working electrodes, graphite (S=0.64 cm^2) and zinc (S=2 cm^2), were mechanically polished with fine emery papers (2/0, 3/0 and 4/0, respectively) and then with polishing

alumina of 1 μm (Banner Scientific Ltd.) on the polishing cloths (Buehler Ltd.). After mechanical polishing the traces of polishing alumina were removed from the electrode surface in an ultra-sonic bath during 5 min. The electrochemical measurements were carried using a PAR 273A potentiostat controlled by a computer through a GPBI PC2A interface.

3. Results and discussion

On Fig. 1. comparison of zinc deposition-dissolution on graphite electrode from chloride and chloride/citrate containing electrolytes are shown. As it can be seen from chloride electrolyte, deposition processes starts at potentials around –1 V, thought one well defined peak, at –1.17 V, after at potentials more negative than –1.4 V proceed simultaneous zinc deposition and hydrogen evolution reactions. In anodic direction, zinc dissolution occurs at potentials more positive than –1 V through one pack and one shoulder. In citrate/chloride electrolyte deposition-dissolution reaction is shifted for ~0.15 V in negative direction and diffusion limited peak is two times smaller, than in chloride electrolytes. This behavior could be explained by zinc ions complexation and lowering of the free zinc ions activity, as well as diffusivity of zinc citrate complex comparing with chloride electrolyte.

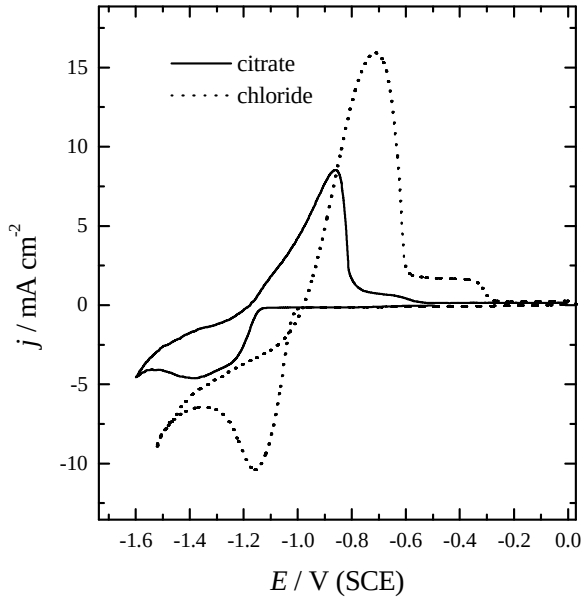

Fig. 1. Cyclic voltammograms of graphite electrode in 1) 0.50 M NH_4Cl + 0.20 M $ZnCl_2$ and 2) with addition of 0.33 M Na-citrate. Sweep rate 20 mV s^{-1}.

In Fig. 2 micrographs of zinc deposits obtained from chloride and chloride/citrate electrolytes at a constant current density of 3.5 mA cm^{-2} and with deposition charges of 10.5 mA h cm^{-2} are shown.

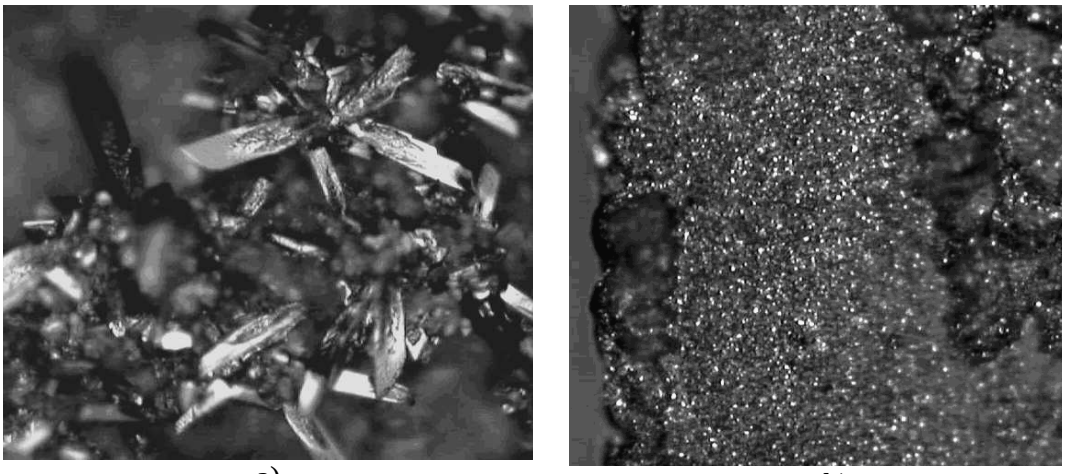

a) b)

Fig. 2. Micrographs of the zinc deposits from a) 0.20 M $ZnCl_2$ + 0.50 M NH_4Cl and b) with addition of 0.33 M Na-citrate.
Deposition current density 3.5 mA cm^{-2}, deposition time 3 h, magnification 200 x.

In chloride electrolyte, Fig. 2a, obtained deposits are practically completely dendritic, so potential risk of fast dendrite growth through separator, during the longer charging times, and formation of short circuits with cathode is permanently present. On the other hand in chloride/citrate electrolyte, Fig. 2b, deposit is smooth without irregularities even in the edges where local current density due to the current distribution phenomena is higher than at the central surface.

The overpotential and the current density in activation-controlled deposition inside the Tafel region are related by:

$$\eta = \frac{b_c}{2.3} \ln \frac{j}{j_0} \qquad (1)$$

Therefore, increasing b_c and decreasing j_0 leads to an increase in the deposition overpotential at the constant current density. It follows from all available data that the former effect is more pronounced resulting in deposits with a finer grain size with decreasing value of the exchange current density.

This analysis explain differences in deposit morphology for chloride and chloride/citrate electrolytes taking into account that Tafel slopes are –35 and –108 mV dec^{-1}, and exchange current densities are 0.38 and 0.027 mA cm^{-2}, respectively. Hence, in chloride electrolyte at 3.5 mA cm^{-2} deposition overpotential is only –30 V, while in chloride/citrate electrolyte is –220 mV.

Insert of Fig. 3. shows the galvanostatic curve for polymerization of aniline from solution containing 0.10 M HCl and 0.10 M aniline monomer on graphite electrode at current density of 1 mA cm^{-2} with polymerization charge of 0.3 mA h cm^{-2}. Polymerization starts at potential of 0.75 V and proceed in the potential range between 0.75 and 0.7 V. After polymerization, electrode was washed with bidistiled water and transferred in the three compartment electrochemical cell with chloride or chloride/citrate electrolyte. After transfer, electrode was conditioned at potential of –0.8 V for 600 s and cyclic voltammograms in the potential range between –0.8 and 0.4 V were taken as shown in Fig. 4. In anodic direction doping of the anions occur at potentials more positive than –0.2 V, with pronounced peak at 0.15 V. In cathodic direction dedoping of anions occur through one shoulder in the potential range of 0.4 to 0.05 V and one well defined peak with the maximum at –0.1 V. Dedoping of anions is finished at potentials of –0.4 V. Small differences in the shapes of cyclic

voltammograms between chloride and chloride/citrate electrolytes, could indicate that only chloride anions are involved in doping/dedoping reaction.

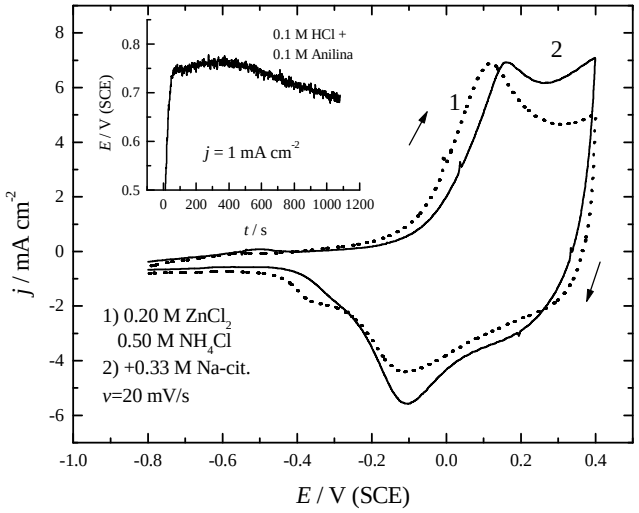

Fig. 3. Cyclic voltammograms of PANI electrode in 1) chloride and 2) chloride/citrate electrolyte (v=20 mV s^{-1}). Insert: galvanostatic curve for aniline polymerization from 0.1 M HCl and 0.1 M aniline at 1 mA cm^{-2} on graphite electrode.

Figure 4. shows charge-discharge curves in chloride and chloride/citrate electrolytes at current density of 0.25 mA cm^{-2}. Charging curves in both solutions are practically identical, but discharging curve in chloride/citrate solution have higher discharge potentials and longer discharge time. Up to now we do not have explanation for that kind of behavior.

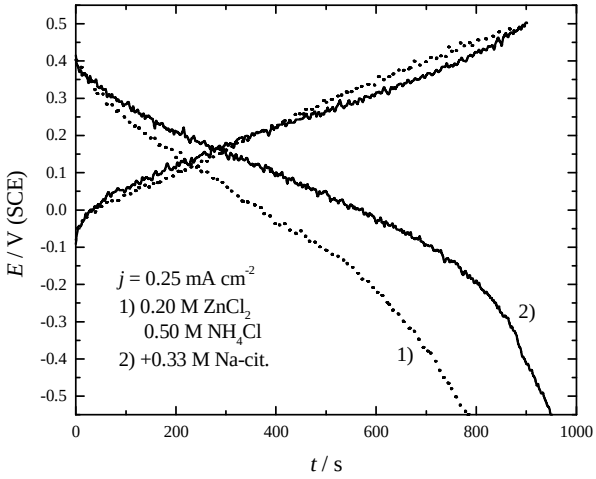

Fig.4. Charge-discharge curve for 1) chloride and 2) chloride/citrate electrolyte at current density of 0.25 mA cm^{-2}.

Charging/discharging characteristics of PANI film electrode are affected with applied current density, mainly because chloride anions diffusion limitation through PANI film. Charging/discharging reaction, assuming that only chloride anions are involved, can be given with following scheme [7]:

$$\text{PANI} + n\text{Cl} \underset{\text{discharge}}{\overset{\text{charge}}{\rightleftharpoons}} \text{PANI(Cl)}_n + ne \qquad (3)$$

On Fig. 5 dependence of capacity during discharge processes for different discharging current densities are shown.

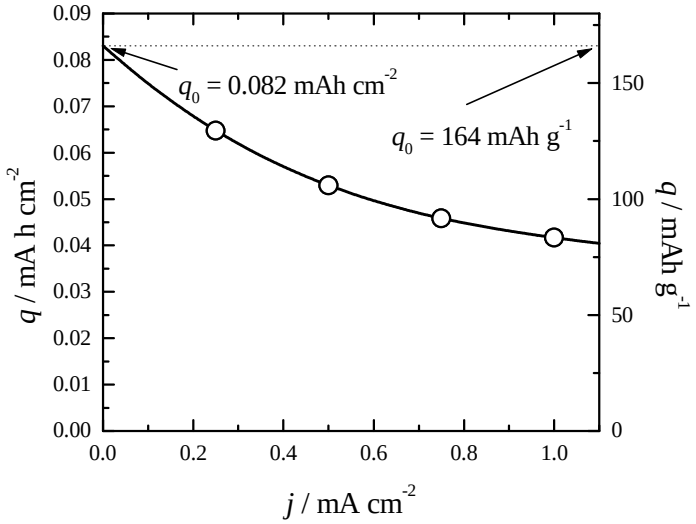

Fig. 5. Dependance of charge (left) and specific charge (right) at different discharge current density for PANI electrode in chloride/citrate electrolyte.

Discharge capacity increase with decreasing applied current density and for the limiting case when $j_d \rightarrow 0$, discharge capacity has a value of 0.082 mAh cm^{-2}.

Assuming the 100% current efficiency during the polymerization of aniline and using the equations [8]:

$$m = \frac{jt\left(M_m + yM_a\right)}{(2+y)F} \qquad (4)$$

It could be calculated that mass of the PANI on graphite electrode was approximately 0.5 mg. Hence, for the limiting case with discharge capacity of 0.082 mAh cm^{-2} specific discharge capacity could be estimate on 165 mAh g^{-1}. In the range of investigated current densities of 0.25 to 1 mA cm^{-2}, specific discharge capacity was in the range of 130 to 85 mAh g^{-1}, respectively.

Acknowledgments

This work is supported by the Ministry of Science and Environmental protection, Republic of Serbia, contract No. 142044.

References

1. Arsov LD, Plieth W, Kossmehl G., J. Solid State Electrochem., 6(1998)355.
2. H. N. Dinh, J. Ding, S.J. Xia, V. I. Birss, J. Electroanal. Chem, 459(1998)45.
3. M.S. Rahmanifar, M.F. Mousavi, M. Shamsipur, M. Ghaemia, J. Pow. Sources, 132(2004)296.
4. J. Kan, H. Xue, S. Mu . J. Pow. Sources, 74(1998)113.
5. G. Mengoli, M.M. Musiani, D. Pletcher, S. Valcher, J. Appl. Electrochem., 17(1987)515.
6. E. Erdem, M. Saçak, M. Karakişla, Polymer International, 39(1996)153.
7. A. Mirmohseni, R. Solhjo, European Polymer Journal, 39(2003)219.
8. J. Kankare, in: D. Wise, G.E. Wnek, D.J. Trantolo, T.M. Cooper, J.D. Gresser (Eds.), Electrical and Optical Polymer Systems: Fundamentals, Methods, and Applications, Marcel Dekker, New York, 1998, Ch.6.